Int. J. Electrochem. Sci., 15 **(2020)** 9013 – 9023, doi: 10.20964/2020.09.25

International Journal of
ELECTROCHEMICAL
SCIENCE
www.electrochemsci.org

Study on the Application of Carbon-coated Copper Foil as Negative Current Collector for Silicon-based Lithium-ion Batteries

Xiaohui Shen[*], *Le Shao, Zhanyuan Tian, Zhaowen Hu, Guolin Cao*

Shaanxi Coal Chemical Industry Technology Research Institute Co., Ltd., Xi'an 710065, Shaanxi, China
[*]E-mail: shenhui06@163.com

Received: 6 April 2020 / *Accepted:* 1 June 2020 / *Published:* 10 August 2020

$LiNi_{0.8}Co_{0.1}Mn_{0.1}O_2$ (NCM811)/SiO_x-Graphite (SiO-C) cell is one of the most potential battery systems with high specific capacity, however, it is difficult to improve its poor cycling performance in practical application. A carbon coated copper foil severed as negative current collector is developed and the effect of conductive carbon film on silicon-based negative electrodes is studied. The main properties of NCM811/SiO-C pouch cells with 9.5 Ah are also compared by using bare copper foil and carbon coated copper foil. The results show that the using of carbon coated copper foil current collector have favorable impact on the rate performance of batteries in particular at higher rates, even can obviously improve the cohesiveness between the anode powder and the current collector, boosting the cycle life. The capacity retention of the batteries with carbon coated copper foil after 300 cycles at 1 C rate is 89.5%, increasing by 5.2% compared with the batteries with bare copper foil.

Keywords: carbon coated copper foil; pouch battery; rate performance; cycle life; capacity retention

1. INTRODUCTION

With the widespread adoption of pure electric vehicles (PEVs) by consumers, elevated driving range has been paid more and more attentions, which is closely related to the energy densities of lithium ion batteries (LIBs)[1,2]. Recently, a large number of advanced negative materials with high capacity and long service life have been applied to store more energy in the cell in order to meet the requirements of modern automotive applications. Silicon (Si) has been widely recognized as an ideal candidate for LIBs negative material with high energy densities, owing to its high theoretical specific capacity and abundant availability. Unfortunately, silicon severed as anode material in commercial LIBs is suffering from a huge volume expansion (~300%) upon full lithiation, which leads to severe pulverization of Si anode materials, following by delamination of the electrode away from the current collector. The resulted

rapidly declining capacity and poor reversibility of Si hamper its practical application [3-7]. Silicon/carbon (Si/C) composites combining high capacity of silicon to good cyclability of carbon have attracted a large quantity of attentions as promising negative electrode materials. Most of strategies in Si/C composites are focused on the size and structure of Si particles, innovative structure designs and synthetic routes of Si/C composites and so on[8-11]. In addition, the research on electrode and even battery designing and manufacturing is also paid many attentions in order to further enhance the specific capacity and cycle stability of Si/C composites based LIBs, such as developing suitable conductive additives and binders, adjusting areal density and compacted density for electrodes, and also optimizing electrolyte and formation process[12-18].

Current collector is a significant component of LIBs as well, the purpose of current collector is to hold electrode integrity and establish an electric contact with a current output. The weak adhesion between electrode materials and current collector would lead to poor cycling performance because of the large volumetric change of Si during charging/discharging, and thus results in poor electrical connection between active materials and current collector[19,20].

In the present work, a novel strategy that a conductive carbon layer enhanced interface between the anode and current collector is constructed by applying carbon coated copper foil as current collector. Herein, pouch cells with capacity of 9.5 Ah containing $LiNi_{0.8}Mn_{0.1}Co_{0.1}O_2$ (NCM811) cathode, silicon dioxide/graphite (SiO/C) composite anode and carbon coated copper foil current collector were fabricated and the electrochemical performance is investigated and compared with the cells with bare copper foil as current collector.

2. EXPERIMENTAL

2.1 Preparation of the pouch cells

The preparation of carbon coated copper foil was conducted by a simple method, conductive carbon along with resin binder was coated on the copper foil surface by an intaglio printing process. The positive electrode was prepared by slurrying NCM811 (RONBAY Technology Introduction Ltd., China) powder with 1.5 wt.% Super-P as conductor and 1.5 wt.% polyvinylidene fluoride (PVDF) as binder in N-methyl-2-pyrrolidone (NMP) solvent, then coating and drying the mixture onto aluminum foil current collector with a thickness of 118 μm. The SiO-C powder (BTR New Energy Material Ltd., China) for negative electrode was slurried with 1.0 wt.% Super-P as conductor and 1.5 wt.% sodium carboxymethyl cellulose (CMC-Na) and 2.0 wt.% styrene butadiene rubber (SBR) as binder in deionized water, which was coated onto bare copper foil and carbon coated copper foil, respectively, with a thickness of 132 μm and 133 μm. After drying at 80ºC for 24 h in a vacuum oven, electrode pieces were tailored according to designed size to assemble pouch cells in a glove box. The positive electrode and negative electrode were separated by a ceramic-coating polypropylene based separator. A commercial liquid electrolyte with the coefficient of 3.5 $g \cdot Ah^{-1}$ was injected in the pouch cells and spread uniformly. The total theoretical capacity per cell was 9.5 Ah.

2.2 Characterization

The surface and cross-sectional morphology were investigated with Hitachi S-4800 Field Emission Scanning Electron Microscope (FESEM). A four-probe meter (ST2253, Suzhou Jingge Electronic., Ltd., Suzhou, China) was employed to evaluate the contact electrical resistivity of SiO-C electrode in stationary state. 180° peel tests were carried out on a universal testing machine (AG-Xplus) with a 10 N load cell at a speed of 50 $mm \cdot min^{-1}$. Electrochemical impedance spectroscopy (EIS) measurement of CR2025 coin cells was also performed using a PARSTAT 4000A electrochemical workstation (Princeton Applied Research) at a scan rate of 0.1 $mV \cdot s^{-1}$.

Electrochemical characterizations were performed at 25ºC, at different current rates ranging from 0.2 C to 5 C. Charges were operated at 1 C in a CC-CV mode until the voltage arrived 4.2 V and the current arrived C/20. High-temperature test was performed under conditions of charging at 1 C-rate (25ºC), resting at 60ºC for 5 h and with that discharging at 1C-rate (60ºC) until the voltage reaches 2.75 V, whereas the low temperature test was carried out by charging the cell at 1 C-rate (25ºC), resting at -20ºC for 24 h, and discharging it at 1 C-rate (-20ºC) until the voltage reaches 2.5 V. Charge/discharge performance tests were conducted on a LAND battery testing system (LAND Electronics Co., Ltd., Wuhan, China). The cells were charged and discharged over a voltage range of 2.75-4.2 V at a current rate of 1 C.

The pouch cells were discharged at 0.2 C and the cut-off voltage was 2.75 V, followed by being disassembled in an Argon-filled dry box. These NCM811/SiO-C pouch cells contained 13 bifacial cathodes and 14 bifacial anodes. The cathode/anode pairs in the middle of the full cells were selected for analysis. N-Methyl-2-pyrrolidone (NMP) was employed to remove the active coating on one side of electrodes separated from pouch cells. The CR2032 SiO-C-Li metal coin half-cells with Celgard 2400 separator (18mm) in 1 M $LiPF_6$ (ethylene carbonate: dimethyl carbonate: ethyl–methyl carbonate = 1:1:1, by volume%) solution were then assembled under argon atmosphere. The capacity of lithium de/re-intercalation into SiO-C electrodes recovered from aged cells was investigated. The nominal specific capacity of coin half-cell was 500 $mAh \cdot g^{-1}$ with the voltage range of 0.01-2.0 V. The initial SiO-C coin half-cells based on fresh SiO-C electrodes were assembled for comparison.

3. RESULTS AND DISCUSSION

Carbon coated copper foil was fabricated by coating and drying the solution with conductive carbon and resin binder onto bare copper foil surface. According to the scanning electron microscopy analysis in Fig.1(a) and (b), the carbon particles about 15-20 nm were well dispersed on the bare copper foil with smooth surface morphology, hence a rough surface and porous structure was constructed by conductive carbon particles, giving rise to an increased contact area between active materials and current collector to a certain extent. Besides, the resin binder severed as bridges to interconnect carbon particles could be able to enhance adhesive attraction of the interface. Fig.1(c) and (d) were the surface and cross-sectional images of SiO-C electrode, the active material particles were uniformly distributed without any

cracks.

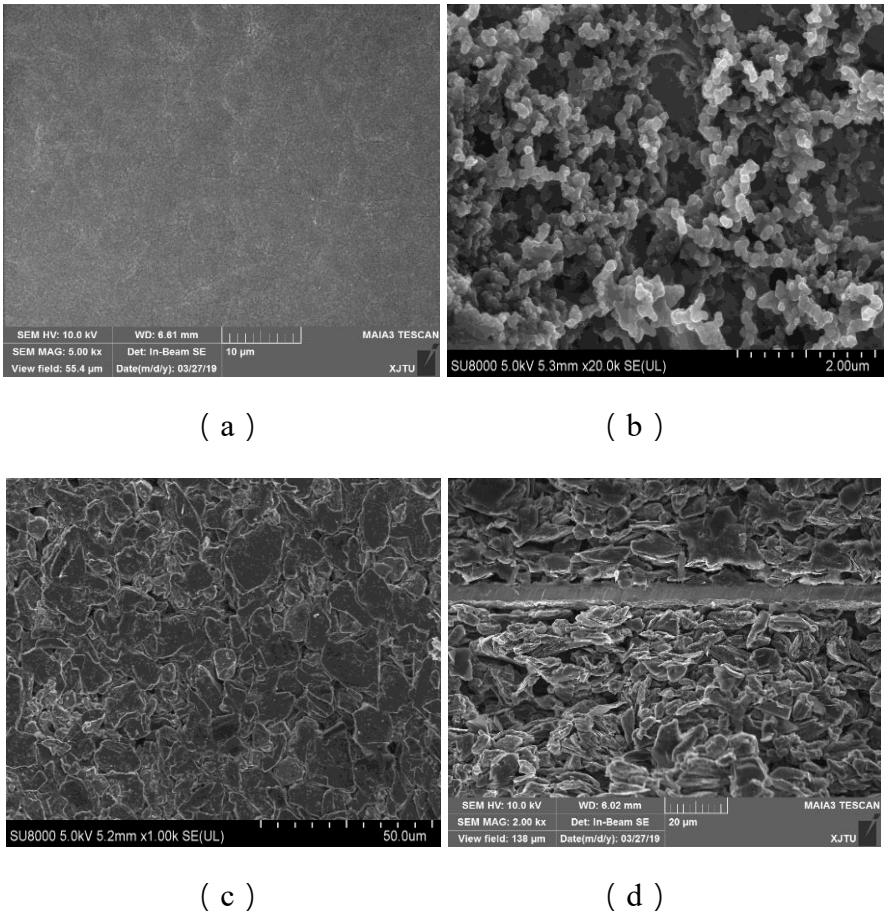

Figure 1. Representative SEM micrograph of (a) bare copper foil and (b) carbon coated copper foil; Plan-view (c) and cross-section (d) of SiO-C electrode.

Table 1. The specific resistance and peel strength of the anodes with bare copper foil and carbon coated copper foil

	Specific Resistance (mΩ·cm)	Peel Strength ($N \cdot m^{-1}$)
Bare copper foil	21.4	17.2
Carbon coated copper foil	19.6	20.3

When using the current collector after the modification of conductive carbon layer in batteries, information of electrical conductivity and peel strength was critical. Thus, the peel strength and electrical conductivity of SiO-C electrode were measured by 180° peel tests and a four-point probe method. The experiments were repeated three times for each sample and the repeated experiments showed consistent values (Table 1). Clearly, the average peel force removing the SiO-C coating layer away from the bare copper foil was only 17.2 $N \cdot m^{-1}$. However, the adhesion between carbon coated copper foil and SiO-C

was enhanced with the peel strength increasing to 20.3 $N \cdot m^{-1}$. For SiO-C electrode, the electrical conductivities increased with the introduction of carbon film. For example, the electrical resistivity of the SiO-C electrode with bare copper foil was 21.4 mΩ·cm, whereas that of the electrode with carbon coated copper foil was 19.6 mΩ·cm. The large increase of electron and ion mobility with the increasing contact area between the current collector and the active material was benefited from the porous carbon film decreased their electrical resistivity [21]. In addition, the addition of coating carbon was beneficial to improve the bonding strength between the copper foil and the SiO-C material [20], so as to improve the stability of the cell and construct a good foundation for the cell to obtain excellent cycling stability and long cycling life.

Fig.2 showed the charge-discharge curves of the bare copper foil and carbon coated copper foil cells at 0.2 C. The discharge capacity, initial coulombic efficiency and specific capacity (based on the weight of NCM811) of bare copper foil and carbon coated copper foil cells were shown in Table 2. The curves of the charge-discharge curves for bare copper foil and carbon coated copper foil cells were similar, but the polarization of bare copper foil cell at initial stage was a little larger compared to carbon coated copper foil cell, because the electrical conductivity of bare copper foil electrode was inferior to that of carbon coated copper foil electrode. It could be concluded that the presence of coating carbon increased the contact area between current collector and SiO-C, facilitating the movement of Li-ion and electrons. Although the electrical conductivity of bare copper foil electrode was lower than that of carbon coated copper foil electrode, the discharge capacity and coulombic efficiency of bare copper foil cell were higher than those of carbon coated copper foil cell. The initial discharge capacity and coulombic efficiency of bare copper foil and carbon coated copper foil cells were 9.543 Ah and 9.517 Ah, 78.1% and 78.0%, respectively. The slightly lower irreversible capacity of carbon coated copper foil cell than bare copper foil cell was mainly originated from the irreversible loss of Li^+ trapped in the introduced carbon coatings of copper foil. The results implied that using carbon coated copper foil instead of pure copper foil had little influence on irreversible capacity or active Li^+ loss in the initial cycle.

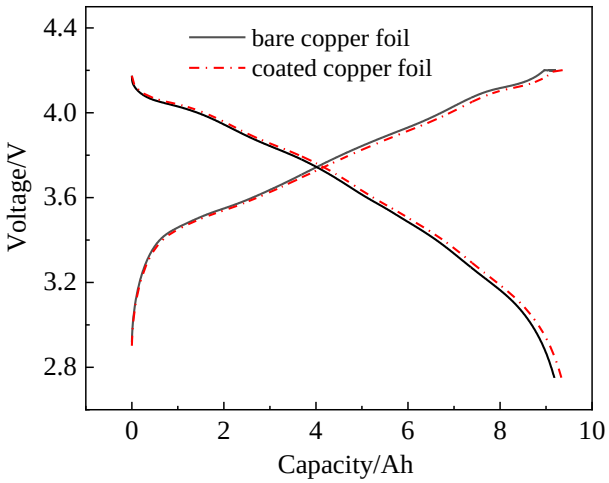

Figure 2. Charge-discharge curves of bare copper foil and carbon coated copper foil cells at 0.2 C.

Table 2. The discharge capacity, initial coulombic efficiency and specific capacity of the bare copper foil and carbon coated copper foil cells.

	Discharge capacity ($mAh \cdot g^{-1}$)	Initial Coulombic Efficiency (%)	Specific capacity ($mAh \cdot g^{-1}$)
Bare copper foil	9.543	78.1	182.5
Carbon coated copper foil	9.517	78.0	182.1

The rate performance of bare copper foil and carbon coated copper foil cells could be observed by plotting the relative capacity against different discharge currents. And the rate performance of the prepared pouch cells with different copper foils was evaluated by charging at 1 C and discharging at various currents from 0.2 C to 5 C. The effect of different discharge currents on voltage–capacity profiles was exhibited in Fig.3. As could be seen, both voltage and capacity were decreased moderately with the discharge current increasing form 0.2 C to 3 C, and a significant decrease of relative capacity appeared as soon as the discharge rate was further increased to 4 C and 5 C. This phenomenon could be interpreted by the electric polarization owing to the increase in the IR drop[22].

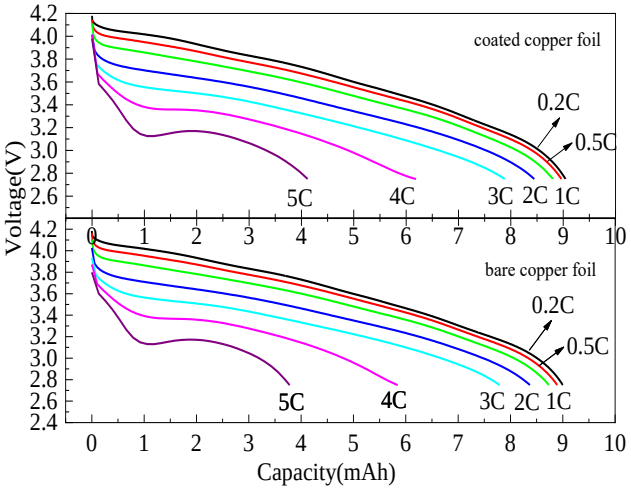

Figure 3. Investigation of the rate capability of bare copper foil and carbon coated copper foil cells.

Although the analogous charge-discharge curves were displayed, the carbon coated copper foil cell exhibited higher specific capacities, particularly at 4 C and 5 C current density [23]. Further increase in discharge rate leaded to a significant decrease in the relative capacity. It was observed that the carbon coated copper foil cell retained the higher relative capacity than the bare copper foil cell as the discharge rate increased to 4 C and 5 C, which was related to the improved conductivity and thus the reduced contact resistance. The relative capacities of carbon coated copper foil cells at the 4 C and 5 C rates were 68.4% and 45.5%, respectively. In contrast, those of bare copper foil cells were 65.0% (4 C) and 42.0% (5 C). It was notable that carbon coated copper foil could improve rate performance to a certain degree, especially at higher rates [24].

Fig.4(a) compared discharge curves of bare copper foil cell and carbon coated copper foil cell at

-20ºC. There was a sharp operating voltage decay in the early stage of discharge process at low temperature. Such obviously decreased voltage could be ascribed to the decreased ionic conductivity of electrolyte arising from its increased viscosity, the limited lithium ion solid diffusion, and a slowdown of cell electrochemical reactions. Furthermore, these two discharge voltage profiles overlapped each other to a large degree and no drag inflection points appeared in both batteries indicating a better low temperature performance.

Fig.4(b) revealed that the relative capacity of carbon coated copper foil cell, which was defined as a percentage of the capacity at -20ºC to the capacity at room temperature, was slightly higher than that of bare copper foil cell, whether the cut-off voltage was 2.75 V or 2.5 V. For example, the discharge capacity ratio of carbon coated copper foil and bare copper foil cells were 79.74% and 78.72% at 2.75 V, and 85.75% and 84.42% at 2.5 V, respectively. At 60ºC, the discharge capacity ratio of carbon coated copper foil was close to that of bare copper foil, which were both over 100%. The promoted discharge capacity could be explained by the increased conductivity of electrolyte and the reduced electrochemical reaction resistance with the rising temperature.

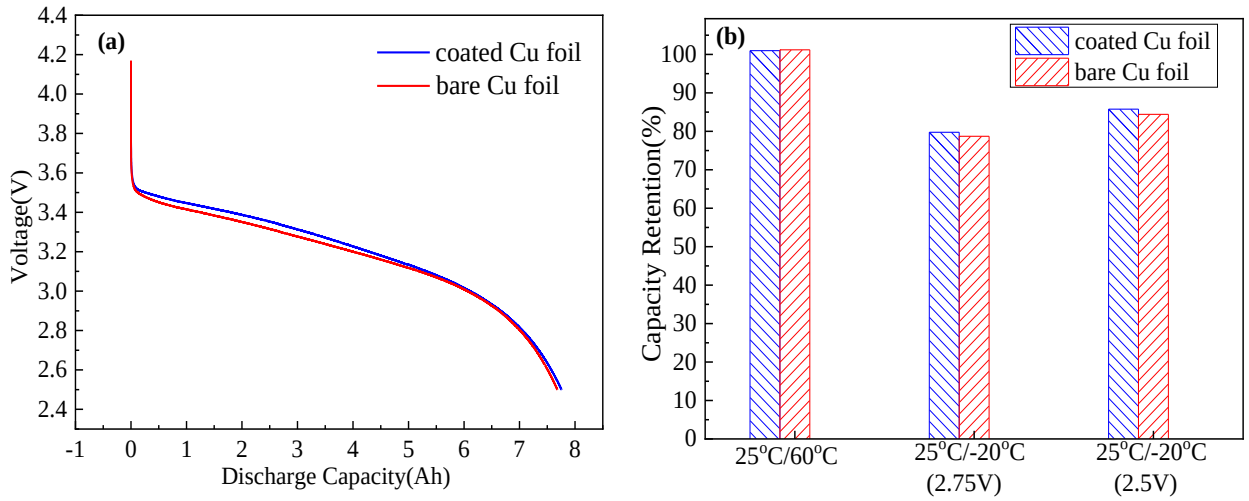

Figure 4. (a) The discharge curve of the bare copper foil and carbon coated copper foil cells at -20℃; (b) Discharge capacity percentage of the bare copper foil and carbon coated copper foil cells at -20℃ and 60℃ to the one at 25℃.

Fig.5 showed the Nyquist plots of electrochemical impedance spectrum (EIS) for carbon coated copper foil and bare copper foil full cells after a pre-charge and 300 cycles. Both of them exhibited a slope line and an inductive loop at low and high frequency, respectively, while two overlapped semicircles appeared at high to middle frequency. Moreover, the surface layer (SEI film) resistance (R_{SEI}) of the electrodes could be reflected by the semicircle at high frequency, the charge-transfer resistance (R_{ct}) was reflected by the semicircle at medium frequency and the electrolyte, separator, and electrodes bulk resistance (R_s) was reflected by the intercept of the semicircle at the far high-frequency end on the real impedance axis [25-28]. As to the warburg impedance, describing Li^+ diffusion on the interface between electrolyte and active materials, was corresponding to the slope line at low frequency. It was clearly that all the resistance values (R_s, R_{SEI}, and R_{ct}) of carbon coated copper foil cell were lower than that of bare copper foil cell. Especially, the R_s and R_{SEI} values of carbon coated copper foil cell

decreased slightly than that of bare copper foil cell after pre-charge, while the decrease was more pronounced after 300 cycles. The impedance reduction could be attributed to the increase in electrical conductivity and the decrease in the degree of polarization, which were all essentially benefited from the functional carbon layer [29]. Besides, the additional binder was also dedicated to the interfacial stability, which could inhibit the impedance from increasing after cycles.

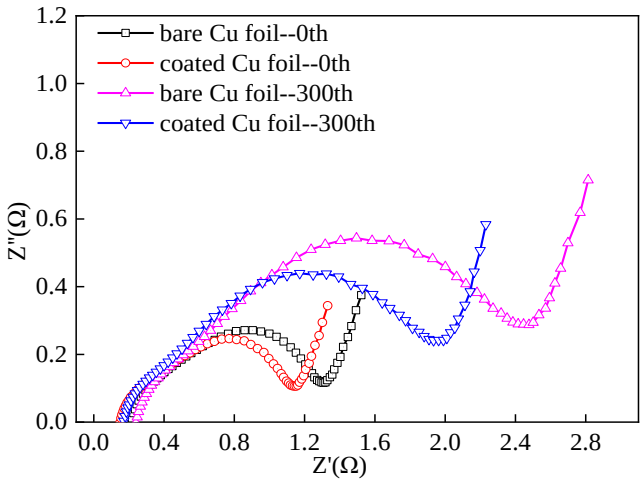

Figure 5. Electrochemical impedance spectra for bare copper foil and carbon coated copper foil full cells before and after 300 cycles.at 1C.

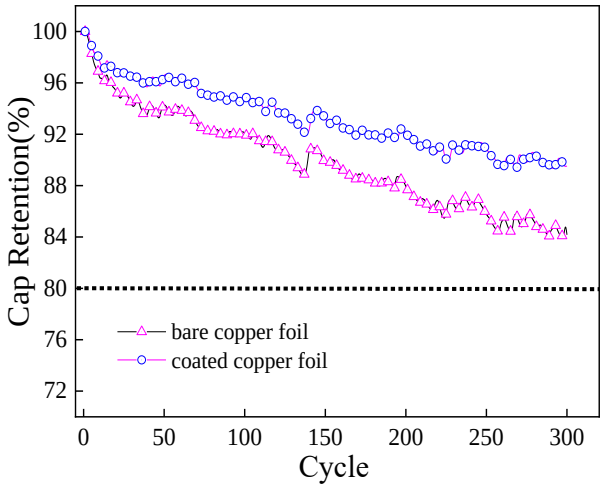

Figure 6. Cycle performance of bare copper foil and carbon coated copper foil cells at ambient temperature.

Fig.6 showed the cycle performance of carbon coated copper foil and bare copper foil cells with a current density of 1 C at ambient temperature. The 1st cycle discharge capacities for the carbon coated copper cell and the bare copper foil cell were 8.58 Ah and 8.61 Ah, while the coulombic efficiencies of them were 95.92% and 96.18%, respectively. As it has been discussed above, the higher reversible capacity of carbon coated copper foil cell than bare copper foil cell was due to an interaction of carbon layer on the copper coil with lithium ion, resulting in an irreversible loss of Li-ion. Whereas, the carbon coated copper foil cells still retained approximate 90% of initial capacity after 300 cycles, whereas bare

copper foil cells only exhibited the capacity retention of 84%, in sharp contrast to less than ~6% capacity retention for carbon coated copper foil cell. The data shed light on that the introduction of functional carbon coating could contribute to a distinctly elevated cycle stability.

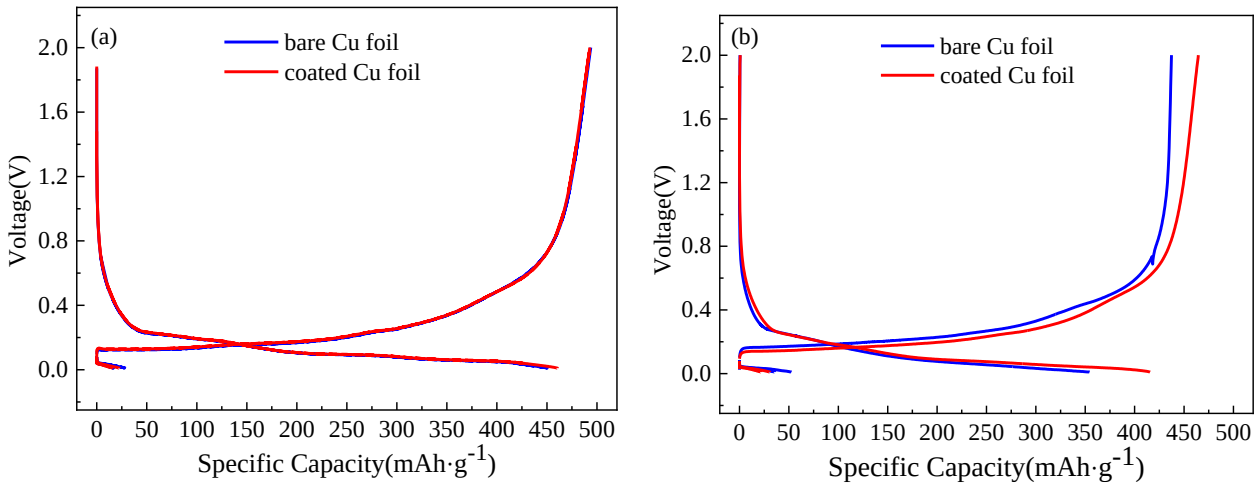

Figure 7. Curves of voltage vs. charge/discharge capacity of SiO-C coin cells with bare copper foil and carbon coated copper foil before (a) and after a pre-charge of 300 cycles (b).

Fig.7 showed the change/discharge profiles of anode electrodes with bare and carbon coated copper foils before and after cycling. The fresh anode with bare copper foil and carbon coated copper foil displayed an initial reversible capacity of 493.5 $mAh \cdot g^{-1}$ and 492.9 $mAh \cdot g^{-1}$, respectively. The specific capacity for the cycled electrode with carbon coated copper foil was 453.2 $mAh \cdot g^{-1}$, which meant it lost 39.7 $mAh \cdot g^{-1}$ of its capacity after 300 cycles. The anode electrode with bare copper foil following the 300th cycle delivered 428.5 $mAh \cdot g^{-1}$, implying that the capacity decay was 65.0 $mAh \cdot g^{-1}$. The result proved that enhanced cycling stability of the anode electrode was obtained at the presence of carbon coated copper foil.

4. CONCLUSION

The carbon coated copper foil severed as current collector for SiO-C electrodes in lithium-ion batteries is investigated. It is found that the SiO-C electrodes with carbon coating copper foil have shown lower specific resistance, better peel strength than the electrode prepared with bare copper foil. Carbon coating copper foil cells have exhibited a little better rate and high/low temperature capability performance. It must be noted that the carbon coating copper foil can promote cycle performance of cells, which exhibit an increased capacity retention of ~6% at 1 C after 300 cycles. The impedance analysis indicates that SiO-C electrodes with carbon coated copper foil possesses a higher ionic conductivity in particular after 300 charge/discharge cycles. And a higher discharge capacity of the additional carbon layer modified SiO-C electrodes is also acquired after 300 cycles, which is in good agreement with that of the pouch cells. It is demonstrated that the carbon coated copper foil current collector can withstand the large volume change of Si-based anodes, because of the functional carbon

layer providing an increased electrical contact within the electrode active materials and a strong polymeric binder-active particle interface. Additionally, the influence of different conducting materials and binders for the copper foil current collector on the electrochemical performance of the Si-based cells should be further investigated.

ACKNOWLEDGMENTS
The authors thank the financial support of the key R&D program of Shaanxi province (Grant No. 2017 ZDCXL-GY-08-03).

References

1. J.B. Goodenough, K.S. Park, *J. Am. Chem. Soc*., 135 (2013) 1167.
2. J. Hassoun, K.S. Lee, Y.K. Sun, B. Scrosati, *J. Am. Chem. Soc*., 133 (2011) 3139.
3. G.X. Wang, J.H. Ahn, J. Yao, S. Bewlay, H.K. Liu, *Electrochem. Commun*., 6 (2004) 689.
4. Z.P. Guo, J.Z. Wang, H.K. Liu, S.X. Dou, *J. Power Sources*, 146 (2005) 448.
5. H. Li, X.J. Huang, L.Q. Chen, Z.G. Wu, Y. Liang, *Electrochem. Solid State Lett*., 2 (1999) 547.
6. A. Magasinski, B. Zdyrko, I. Kovalenko, B. Hertzberg, R. Burtovyy, C.F. Huebner, T.F. Fuller, I. Luzinov, G. Yushin, *ACS Appl. Mater. Interfaces*, 2 (2010) 3004.
7. S.H. Yook, S.H. Kim, C.H. Park, D.W. Kim, *Rsc Advances*, 6 (2016) 83126.
8. J. Yang, B.F. Wang, K. Wang, Y. Liu, J.Y. Xie, Z.S. Wen, *Electrochem. Solid State Lett.,* 6 (2003) A154.
9. B.C. Kim, H. Uono, T. Satou, T. Fuse, T. Ishihara, M. Ue, M. Senna, *J. Electrochem. Soc*., 152 (2005) A523.
10. M. Yoshio, S. Kugino, N. Dimov, *J. Power Sources*, 153 (2006) 375-379.
11. X.H. Shen, Z.Y. Tian, R.J. Fan, L. Shao, D.P. Zhang, G.L. Cao, L. Kou, Y.Z. Bai, *J. Energy Chem*., 27 (2018) 1067.
12. T. Miyuki, Y. Okuyama, T. Sakamoto, Y. Eda, T. Kojima, T. Sakai, *Electrochem*., 80 (2012) 401.
13. J. Li, R.B. Lewis, J.R. Dahn, *Electrochem. Solid State Lett*., 10 (2007) A17.
14. S. Komaba, N. Yabuuchi, T. Ozeki, Z.J. Han, K. Shimomura, H. Yui, Y. Katayama, T. Miura, *J. Phy. Chem. C*, 116 (2012) 1380.
15. M.H. Ryou, J. Kim, I. Lee, S. Kim, Y.K. Jeong, S. Hong, J.H. Ryu, T.S. Kim, J.K. Park, H. Lee, J.W. Choi, *Adv. Mater*., 25 (2013) 1571.
16. S. Dalavi, P. Guduru, B.L. Lucht, *J. Electrochem. Soc*., 159 (2012) A642.
17. I.A. Profatilova, C. Stock, A. Schmitz, S. Passerini, M. Winter, *J.Power Sources*, 222 (2013) 140.
18. T. Takamura, M. Uehara, J. Suzuki, K. Sekine, K. Tamura, *J. Power Sources*, 158 (2006) 1401.
19. G.F. Yang, K.Y. Song, S.K. Joo, *Rsc Advances*, 5 (2015) 16702.
20. M. Kuenzel, D. Bresser, G.T. Kim, P. Axmann, M.W. Mehrens, S. Passerini, *ACS Appl. Energy Mater.*, 3 (2020) 218.
21. S.Y. Kim, Y.I. Song, J.H. Wee, C.H. Kim, B.W. Ahn, J.W. Lee, S.J. Shu, M. Terrones, Y.A. Kim, C.M. Yang, *Carbon*, 153 (2019) 495.
22. S.S. Zhang, K. Xu, T.R. Jow, *J. Power Sources*, 140 (2005) 361.
23. M.Z. Wang, H. Yang, K. Wang, S.L Chen, H.N Ci, L.R. Shi, J.Y. Shan, S.P. Xu, Q.C. Wu, C.Z. Wang, M. Tang, P. Gao, Z.F. Liu, H.L. Peng, *Nano Lett.*, 20 (2020) 2175.
24. M.S. Yazici, D. Krassowski, J. Prakash, J. *Power Sources*, 141 (2005) 171.
25. S. Wang, X. Xiao, Y. Zhou, C. Fu, S. Jiao, *Electrochim. Acta*, 282 (2018) 946.
26. S.H. Ng, J. Wang, D. Wexler, S.Y. Chew, H.K. Liu, *J. Phy. Chem*. C, 111 (2007) 11131.
27. J. Yang, X. Kang, L. Hu, X. Gong, S. Mu, *J. Mater. Chem*., 2 (2014) 6870.

28. W. Zhang, X. Zhang, L. Chen, J. Dai, Y. Ding, L. Ji, J. Zhao, M. Yan, F. Yang, *ACS Catal.*, 8 (2018) 8092.
29. M.X. Chen, L.W. Cheng, J.C. Chen, Y. Zhou, J.D. Liang, S. Dong, M. Chen, X.T. Wang, H. Wang, *ACS Appl. Mater. Interfaces*, 12 (2020) 3681.